

Equilibrium Disperse-Dye Sorption by Isotactic Polypropylene Films of Varied Thermal Histories

KOICHIRO YONETAKE, TORU MASUKO,* TOMOYUKI SHIMANUKI,
and MIKIO KARASAWA, *Faculty of Engineering, Yamagata University,
Jonan-4, Yonezawa-shi, Yamagata-ken, 992 Japan*

Synopsis

Spherulitic polypropylene (PP) films prepared by a melt-quenched process and then exposed to isothermal annealing treatments at various temperatures ranging from 120°C to 155°C have been dyed at 80°C with C.I. Disperse Yellow 7 (Y-7) or *p*-aminoazobenzene. Different PP films as crystallized isothermally in the range of 60°C to 155°C have also been dyed with the same dyes. The equilibrium dye sorption (M_0) obtained for these films increased slightly with an increase in polymer volume crystallinity (C_v). Using fine structural data of these films, the change in M_0 were analyzed in terms of the mosaic-block structural model; e.g., the values of M_0 were divided into sorption by the amorphous end region (M_e) located between lamella surfaces and sorption by the amorphous side region (M_s) located between crystalline cores parallel to the molecular chain axis. The value of M_s increased with increasing C_v in both cases of the dyeing systems, while the value of M_e decreased monotonically in an opposite manner. The amorphous chains in the side region seem to have a strong affinity to a long rodlike dye molecule of Y-7; this feature is considered to be associated with the extended chain conformation of the side region which originates from distorted lattice chains.

INTRODUCTION

When a hydrophobic fiber, such as poly(ethylene terephthalate) (PET), is dyed with disperse dyes, it has often been observed that the dye uptake by the fiber increases with an increase in its crystallinity.¹⁻³ This seems to contradict a familiar view that a change in dye sorption is closely related to that of fraction of amorphous region involved in the fiber.

This parallel increase between the crystallinity of a fiber and the dye sorption forces us to consider that the fine-structural modification of the fiber, particularly in a molecular level, accompanies some substantial changes in the amorphous region of the fiber, and then it greatly affects development of effective dyeing sites in the fiber. This situation cannot be explained only by variation of the average crystallinity of the fiber. Thus, the change in the equilibrium dye sorption should be expressed by an adequate function including either the crystallinity or the fine-structural parameters, e.g., the long period, the crystallite sizes, and various molecular orientation factors of the fiber.

We have recently communicated that, when isotropic high-density polyethylene films annealed variously at different temperatures were dyed with disperse dyes, they show similar characteristics to that observed in the case of PET fibers.⁴ In order to explain these curious dyeing behaviors, therefore, we have proposed a new dyeing model on the basis of the mosaic block structural

* To whom correspondence should be addressed.

model of polymeric materials⁵ often applied to interpret the viscoelastic properties of crystalline polymers.⁶

In that dyeing model, the amorphous region of a semicrystalline polymer has been divided into two separate regions: one is the amorphous end region composed of fold, cilia, and tie chains, and the other the amorphous side region formed of the amorphous chains with rather extended conformations originating from crystallographic misfits in lattice chains. These two regions are further assumed to have their respective dyeability for disperse dyes. If the polymer is suffered by annealing treatments, the volume fractions of the two regions would vary with the average crystallinity so that this variation governs intensively the possibility of dye sorption.

On a line similar to that of the previous study, the purpose of this work is to test whether or not the mosaic-block dyeing model above-described is available to the dyeing behavior of annealed or crystallized isotactic polypropylene (PP) films dyed with disperse dyes.

APPLICATION OF MOSAIC-BLOCK DYEING MODEL TO POLYPROPYLENE

By extensive studies on deformation of single crystals, several investigators^{7,8} have shown that a well-defined PP single crystal of a lath shape is fractured into small blocks connected to each other with fibrillar bundles of molecular chains. In addition, using an electron microscope, Shii and Ishikawa⁹ have demonstrated that this lath-shaped PP single crystal is originally composed of mosaic crystallite aggregates. Therefore, we may reasonably consider a spherulitic bulk PP film to be comprised of many small mosaic blocks in a fine-structural level, since the spherulites of PP are made of systematically stacked thin lamellae.¹⁰

Alternatively, according to the study on the viscoelastic properties of PP by Wada et al.,¹¹ there are two situations of the amorphous phase within PP spherulites: one is located between the fragments of lamellae (crystallite cores) aligned in the radial direction of the spherulite, and the other between fold surfaces of the lamellae. This view is substantially in agreement with Takayanagi's model of viscoelasticity for a single crystal mat or a bulk state of PE⁶; hence, accepting the above view, we may apply the same mosaic model of dyeing to dyeing behaviors of bulk PP films as already proposed in the case of annealed PE.⁴

Now consider a unit volume of spherulitic bulk PP, the volume crystallinity of which is C_v , which is composed of N blocks of an equal size. Each block of its volume V_b contains the crystallite core of a square pillar in its shape, of which lengths along the molecular axis and perpendicular to that axis are l_c and l_s , respectively, as illustrated in Figure 1. The core is enclosed by the amorphous end region and the side region; the thicknesses of these regions, respectively, are expressed by l_a and h . In reference to the previous work,⁴ the equilibrium dye uptake per 1 g of the polymer M_0 can be expressed by the next form,

$$M_0\rho = (K_s V_s/V_b + K_e V_e/V_b)c \quad (1)$$

where ρ is the density of the dyed polymer, V_s and V_e are the respective volumes of the amorphous side region and the end region, c is the concentration of a dyeing bath, and K_s and K_e are the coefficients corresponding to solubility of a disperse

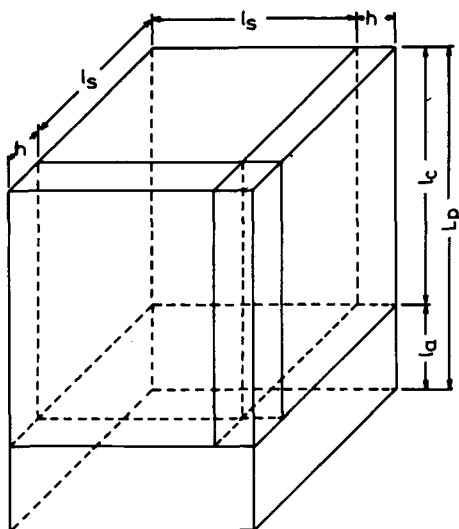


Fig. 1. Schematic representation of a mosaic block assumed.

dye into the side region and the end region, respectively. The coefficient K_s is tentatively assumed to relate the crystallite core length as in the following expression:

$$K_s = l_c \cdot m_s \quad (2)$$

where m_s is the constant independent of both the fine-structural parameters and the dye bath concentration. Utilizing the expressions of V_s and V_e in terms of the fine-structural parameters, we obtain with $p = h/l_c$

$$\begin{aligned} V_c &= l_c l_s^2, & V_e &= (L_p - l_c) l_s^2 \cdot (1 + p)^2 \\ V_s &= l_c l_s^2 \cdot (2 + p) \cdot p, & V_b &= L_p l_s^2 \cdot (1 + p)^2 \end{aligned} \quad (3)$$

The crystallinity C_v is given by

$$C_v = \frac{V_c}{V_b} = \frac{l_c}{L_p \cdot (1 + p)^2} \quad (4)$$

M_0 is distributed in two parts M_s and M_e over the respective volumes V_s and V_e

$$M_0 = M_s + M_e \quad (5)$$

and we find with the help of eqs. (2) and (4)

$$\begin{aligned} M_e &= K_e V_e c / V_b \rho = K_e (1 - l_c / L_p) c / \rho \\ &= K_e [1 - (1 + p)^2 C_v] c / \rho \end{aligned} \quad (6)$$

$$\begin{aligned} M_s &= K_s V_s c / V_b \rho = K_s C_v p (2 + p) c / \rho \\ &= m_s C_v^2 L_p (2 + p) p (1 + p)^2 c / \rho \end{aligned} \quad (7)$$

If L_p , p , and C_v are measurable quantities, then the following variables η and ξ are also calculable:

$$\begin{aligned} \xi &= M_s K_e / M_e m_s \\ &= C_v^2 (2 + p) p (1 + p)^2 L_p / [1 - (1 + p)^2 C_v] \end{aligned} \quad (8)$$

$$\begin{aligned}\eta &= (K_e/M_e)(M_s + M_e)c = M_0\rho/[1 - (1 + p)^2C_v] \\ &= (K_e + m_s \cdot \xi)c\end{aligned}\quad (9)$$

This linear relationship between the measurable quantities η and ξ gives insight into the sorption effects and also proves that, according to eq. (2), K_s is proportional to l_c . A physical signification of eq. (2) will be discussed in a later section.

Through the procedure above, we can at least discuss the partition characteristics of disperse dyes into the side and end regions.

EXPERIMENTAL

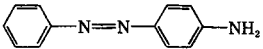
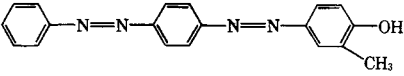
Film Preparation

The sample used in the present study is the unfractionated PP film of a commercial type with its weight-average molecular weight $M_w = 2.62 \times 10^5$ ($\bar{M}_w/\bar{M}_n = 4.2$) and 96% tacticity (a residue of extraction by boiling *n*-heptane). It was hot-pressed into films about 200 μm thick between two ferrotype plates at 230°C and 4.9×10^6 Pa (= 50 kg/cm²) for 10 min, followed by quenching or isothermal crystallization at various selected temperatures ranged from -70°C to 155°C (T_c). The code names of the samples prepared and crystallization conditions applied are shown in Table I. Parts of these films were then iso-

TABLE I
Code Name of Sample Films and Conditions of Film Preparation

Sample	Crystallization		Heating medium	Annealing		Spherulite diameters (μm)
	Temp (°C)	Time		Temp (°C)	Time (min)	
S ₁	-70	5 min	Ethanol + dry ice	150	10	5.4
S ₂	-10	5 min	Ice water + NaCl	150	10	8.2
S ₃₋₁	0	5 min	Ice water	120	30	10.4
S ₃₋₂	0	5 min	Ice water	140	30	10.4
S ₃₋₃	0	5 min	Ice water	150	30	10.4
S ₃₋₄	0	5 min	Ice water	155	30	10.4
S ₄	60	2 h	PEG	150	10	30
S ₅₋₁	80	24 h	PEG	100	30	50
S ₅₋₂	80	24 h	PEG	120	30	50
S ₅₋₃	80	24 h	PEG	140	30	50
S ₅₋₄	80	24 h	PEG	150	30	50
S ₅₋₅	80	24 h	PEG	155	30	50
S ₆₋₁	100	24 h	Air	—	—	75
S ₆₋₂	100	24 h	Air	150	10	80
S ₇₋₁	120	1 Week	Air	—	—	100
S ₇₋₂	120	1 Week	Air	150	10	100
S ₈₋₁	140	2 Weeks	Air	—	—	250
S ₈₋₂	140	2 Weeks	Air	150	10	250
S ₉₋₁	150	2 Weeks	Air	—	—	500
S ₉₋₂	150	2 Weeks	Air	150	10	500
S ₁₀₋₁	155	4 Weeks	Air	—	—	1000
S ₁₀₋₂	155	4 Weeks	Air	150	10	1000

TABLE II
 Disperse Dyes Used in the Present Study

Dye (simplified code)	Molecular structures	Molecular weight (obs mp °C)	λ_{\max} (nm) in chlorobenzene
<i>p</i> -Aminoazo- benzene (PAAB)		197.3 (124)	377
C. I. Disperse Yellow 7 (Y-7)		316.4 (157-158)	385

thermally annealed in hot poly(ethylene glycol); the annealing temperatures (T_a) employed spanned the range from 100°C to 155°C.

On quenched samples of S_1 , S_2 , and S_3 , spherulitic entities were observed by a small-angle light-scattering (SALS) method using an He-Ne gas laser; the diameters of the spherulites in these films were evaluated from the H_v patterns of SALS by the Stein-Rhodes equation.¹² On the other hand, the spherulite sizes of the samples crystallized at more than 0°C were determined by use of a polarizing microscope. The values of these diameters obtained are also shown in Table I.

Dyeing

Disperse dyes used and some of their characteristics are shown in Table II. These dyes were purified by repeated recrystallization from water or a mixture of water and methanol (1:1). The dyeing apparatus used in the present study was similar to that described in the previous paper.⁴ The composition of dye baths and dyeing conditions utilized are shown in Table III. According to our preliminary experiments, every dye sorption equilibrium observed in all the samples had come up after dyeing time of 50 h at 80°C. The dyes sorbed by the films were stripped with chlorobenzene at 70°C, and the amount of them in this solvent was determined from the optical density of the solution at the maximum wavelength by use of a Hitachi 124 Spectrophotometer. The first column of Table IV shows the values of the equilibrium dye sorption obtained for the sample films.

TABLE III

Dye	<i>p</i> -Aminoazobenzene	C. I. Disperse Yellow 7
Weight of dye (mg)	250	40
Neugen HC ^a (g)	—	1
Deionized water (liter)	2.5	2.5
Dyeing temp (°C)	80	80
Dyeing time (h)	50	50

^a Neugen HC is the commercial name of a nonionic surfactant supplied by Dai-ichi Kogyo Seiyaku Co., Ltd.

TABLE IV
Equilibrium Dye Uptakes and Fine-Structural Variables of Dyed Samples

Sample	M_0 (mg dye/g polymer)		ρ (g/cm ³)	C_v	L_p (Å)	l_{110} (Å)	l_{040} (Å)
	Y-7	PAAB					
S ₃₋₁	0.578	1.057	0.9020	0.422	165	121	136
S ₃₋₂	0.569	1.076	0.9072	0.498	216	141	160
S ₃₋₃	0.643	1.027	0.9128	0.567	274	161	173
S ₃₋₄	0.653	1.080	0.9124	0.579	349	164	182
S ₅₋₁	0.492	1.073	0.9032	0.461	175	147	163
S ₅₋₂	0.511	1.058	0.9039	0.470	178	149	167
S ₅₋₃	0.648	1.112	0.9077	0.519	223	151	168
S ₅₋₄	0.652	1.088	0.9102	0.554	279	162	178
S ₅₋₅	0.660	1.091	0.9131	0.562	337	168	177
S ₆₋₁	0.597	1.191	0.9066	0.501	196	143	180
S ₆₋₂	0.672	1.141	0.9096	0.541	285	168	192
S ₇₋₁	0.647	1.161	0.9102	0.545	241	149	188
S ₇₋₂	0.672	1.152	0.9108	0.561	330	185	199
S ₈₋₁	0.660	1.220	0.9132	0.576	313	175	198
S ₈₋₂	0.705	1.115	0.9134	0.580	372	195	224
S ₉₋₁	0.651	1.204	0.9158	0.585	400	211	238
S ₉₋₂	0.654	1.082	0.9156	0.591	418	219	252
S ₁₀₋₁	0.635	1.168	0.9166	0.591	452	221	245
S ₁₀₋₂	0.638	1.053	0.9170	0.621	474	236	273

Structural Characterization

All the samples structurally examined were dyed ones. Densities (ρ) of the samples were measured at 25°C by use of a density-gradient column filled with a mixture of water and 1-propanol. The values of crystalline dimensions and crystalline weight fractions (C_x) of the samples were determined by X-ray analysis; these measurements were carried out on a Rota Flex RU-3 (Rigaku Denki Co.,) using Ni-filtered Cu-K α radiation generated under the power conditions of 40 kV and 100 mA. It was confirmed by a wide-angle X-ray scattering (WAXS) method that the crystallites of all the samples dyed have only the monoclinic crystalline modification. The value of C_x was calculated by the next equation¹³

$$C_x = \frac{S_c}{1.297S_a + S_c} \quad (10)$$

where S_c is the sum of integral WAXS intensities of (hkl) planes located in the range from $2\theta = 7^\circ$ to $2\theta = 33^\circ$, and S_a the intensity of the amorphous scattering which is determined by the Weidinger-Hermans method.¹³ The values of volume crystallinity C_v were approximated by the next relationship,

$$C_v = (\rho/\rho_c)C_x \quad (11)$$

where ρ_c is the crystal density of PP at 25°C, being estimated as 0.9354 g/cm³.¹⁴

From the integral widths (β) of WAXS traces, the crystallite sizes normal to (hkl) planes (l_{hkl}) were calculated by Scherrer's equation¹⁵ with the constant $K = 1.0$. The instrumental broadening was obtained from the width of the

diffraction peak of a sample of hexamethylene tetramine. On that calculation, the Gaussian distribution of the instrumental broadening correction was assumed. The long period L_p was determined photographically by use of a pinhole small-angle X-ray scattering camera; the distance between a specimen and a photographic film was 40.7 cm.

RESULTS AND DISCUSSION

Spherulite Size and Dye Uptake

As shown in Table I, the PP films prepared contain the spherulites of which diameters vary from ca. $5 \mu\text{m}$ to ca. $10^3 \mu\text{m}$. The films annealed at 150°C were dyed with C. I. Disperse Yellow 7 (Y-7) under the same dyeing conditions. The equilibrium uptakes of Y-7 for these films are shown in Table IV. The uptakes for the S_1 and S_2 samples are $0.653 \text{ mg dye/g polymer}$ and $0.654 \text{ mg dye/g polymer}$, respectively. These values are plotted against the diameter of the spherulite in Figure 2. Interestingly, the values remain almost constant, although the diameter of the spherulite increases significantly.

As a result of the study of gas permeation in PE, Michaels and Bixler¹⁶ have presumed that spherulitic structures of crystalline polymers do not impede diffusion of small gas molecules in the substrates. Recently, it has also been reported by Frank and Lehner¹⁷ that a stabilizer, Tinuvin 328, which has a similar molecular size to that of a disperse dye, can penetrate through the spherulitic structures of PP. Thus, we examined our dyed sample in the following manner. After the surface of the dyed S_{10-2} film, composed of the largest spherulites in the present study, was thoroughly rinsed with methanol, then this film was investigated in detail using a polarizing microscope. As a result, whole areas of the film surface and the cross section of the film were homogeneously dyed with Y-7, so that the Y-7 molecules can penetrate easily into the spherulitic structures of PP.

From the findings above, we can safely conclude that penetration and sorption of dye molecules are not hindered by supramolecular structures of crystalline polymers, and the dye molecules are adsorbed by the amorphous molecular chains variously located within the spherulitic structures.

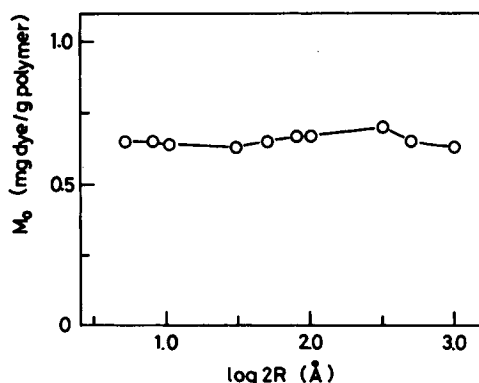


Fig. 2. Change in the equilibrium dye uptake of Y-7 at a dyeing temperature of 80°C against the diameter of the spherulite within PP films.

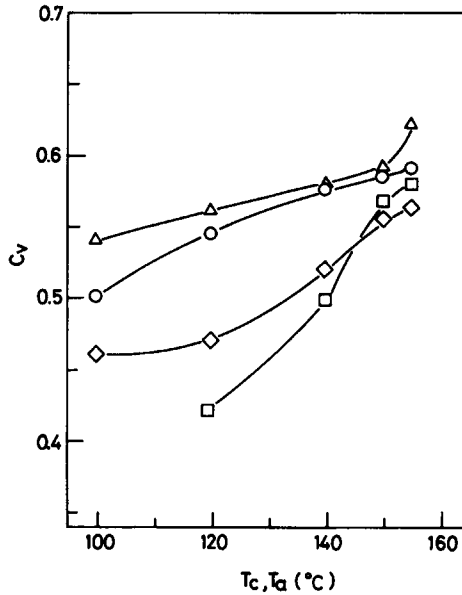


Fig. 3. Changes in crystallinity of the dyed samples as functions of crystallization temperatures or annealing temperatures: (O) for the samples as isothermally crystallized (S₆₋₁, S₇₋₁, S₈₋₁, S₉₋₁, S₁₀₋₁); (Δ) for the samples crystallized and then annealed at 150°C for 10 min (S₆₋₂, S₇₋₂, S₈₋₂, S₉₋₂, S₁₀₋₂); (□) for the samples quenched at 0°C and then annealed at various temperatures (S₃₋₁–S₃₋₄); (◇) for the samples crystallized at 80°C and then annealed at 150°C for 10 min (S₅₋₁–S₅₋₅).

Fine Structural Characterization of Dyed PP Films

The volume crystallinity C_v of the quenched-annealed samples (S₃₋₁–S₃₋₄) and the crystallized-annealed samples (S₅₋₁–S₅₋₅) is plotted against T_a in Figure 3; additionally, C_v of the samples are crystallized at temperatures higher than 100°C (S₆₋₁, S₇₋₁, S₈₋₁, S₉₋₁, S₁₀₋₁) and then annealed at 150°C (S₆₋₂, S₇₋₂, S₈₋₂, S₉₋₂, S₁₀₋₂) are parallely plotted against T_c in the same abscissa of this figure. The values of C_v in respective series increase monotonically with an increase in T_a or T_c . Apparently, the temperature dependences of C_v of these samples clearly differ from each other according to the varied thermal histories of them, so that, as shown in Figure 3, four different curves are obtained. In view of efficiency of crystallization, the values of C_v of the samples are crystallized in the lower temperature range are much larger than those of the samples quenched at 0°C and then suffered by annealing in the range below 150°C; this means that the primary crystallization in the PP film is more effective for improvement of crystallinity than the secondary crystallization (annealing treatments) is. At high temperatures of T_a or T_c more than 150°C, however, the values of C_v have a trend to converge on the maximum value, $C_v = \text{ca. } 0.6$. Annealing treatments of the quenched PP at that temperature range accompany particularly a drastic melt-recrystallization process, which do not substantially differ from the primary crystallization.

In Figure 4, both changes in L_p and l_{hkl} are plotted as a function of C_v . The values of L_p increases with a rise in C_v . Of course, compared with the results shown in Figure 3, these values increase with an increase in T_a . The feature of

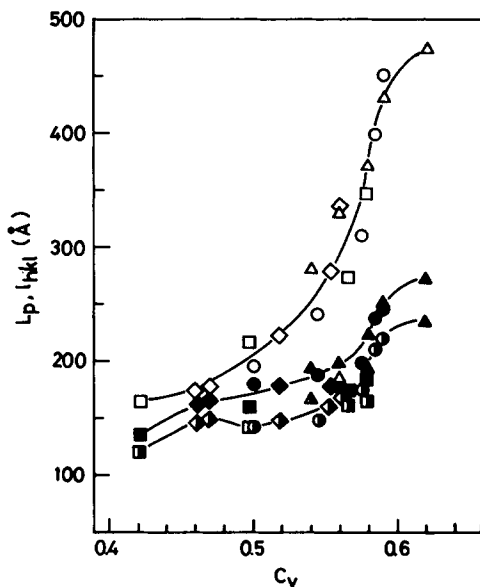


Fig. 4. Changes in long period and crystallite sizes as functions of volume crystallinity: (○, △, □, ◇) for long period; (○, △, □, ◇) for l_{110} ; (●, ▲, ■, ◆) for l_{040} . The marks of circles, triangles, squares, and diamonds correspond to the ones shown in Figure 3.

L_p increasing with T_a is quantitatively consistent with the results by Shii et al.¹⁸ and Wada et al.¹¹ Irrespective of the varied thermal histories of these samples, the relationship between C_v and L_p is indicated by one curve, as shown in Figure 4. Similar relations to this can be observed in the changes in l_{hkl} ; e.g., the values of l_{040} and l_{110} increase with increasing C_v , following respective traces independent of the varied thermal histories. It should be noted, however, that the values of l_{hkl} do not increase as steeply with increasing C_v as do those of L_p . Thus we can deduce that the increase in C_v is ascribable to substantial development of the crystal growth along the molecular axis of this polymer.

Dye Sorption Interpreted by the Mosaic Block Dyeing Model

The equilibrium uptake of Y-7 obtained is plotted against C_v in Figure 5. The values of the uptake of this dye increase slightly with an increase in C_v at the lower range, and remain almost constant at the higher range of C_v . Moreover, a similar relation to this can be observed in the case of PAAB, as indicated in Figure 6. Thus, the changes in the equilibrium dye uptakes do not depend directly on variation of C_v of the annealed PP films.

Therefore, we apply the mosaic block model of dyeing to the above dyeing cases using the additional structural parameters other than C_v , e.g., L_p and l_s . To a first approximation, the value of l_s is replaced by that of $(l_{110} \cdot l_{040})^{1/2}$. The test plots of η vs. ξ are shown in Figure 7. These plots yield fairly good linear relationships below the values of $C_v = 0.58$ in both cases of dye sorption. The lines drawn in Figure 7 are obtained from the least-squares fits of the numerical data. The slopes and intercepts of these lines afford the values of $m_s c$ and $K_e c$, respectively, as described in the preceding section.

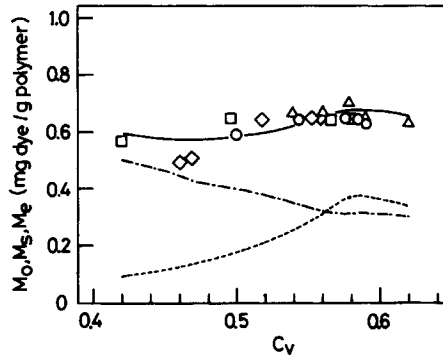


Fig. 5. Variation of the equilibrium dye uptake of Y-7 vs. volume crystallinity. (\circ , Δ , \square , \diamond) Indicate experimental points and the line through these points is a theoretical curve of total sorption (M_0) determined by eq. (5). Theoretical curves of sorption by the side region (M_s) calculated by eq. (7) (---) and by the end region (M_e) determined by eq. (6) (- - -).

Since the experimental points above $C_v = 0.58$ in this figure deviate considerably from the linear relationships of each dyeing case, then the values of the p parameter are so slightly reduced that the numerical values of η and ξ would locate on those lines determined from the data below $C_v = 0.58$. The resulting points so adjusted are also displayed in Figure 7, using different marks. Such deviations above may be due to the abrupt increase of l_{hkl} in the range above $C_v = 0.58$. Thus, we take the view that the value of h decreases slightly with increasing C_v in that range. The values of h associated with the p parameter are plotted against C_v in Figure 8, where they indicate the maximum at $C_v = 0.58$. These values of h lie in the range from ca. 13 Å to 20 Å, being similar to those of PE obtained in the previous work.⁴

Using the values of m_{sc} and K_{ec} determined by the above procedure, the quantities of M_s and M_e of each dye are calculated by eqs. (5), (6), and (7), and

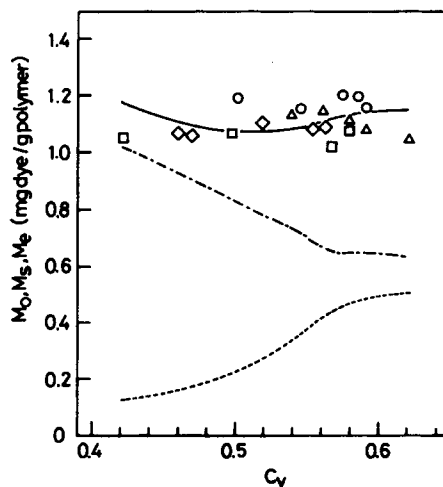


Fig. 6. Variation of the equilibrium dye uptake of PAAB vs. volume crystallinity. The symbols and curves have the same significance as indicated in Figure 5.

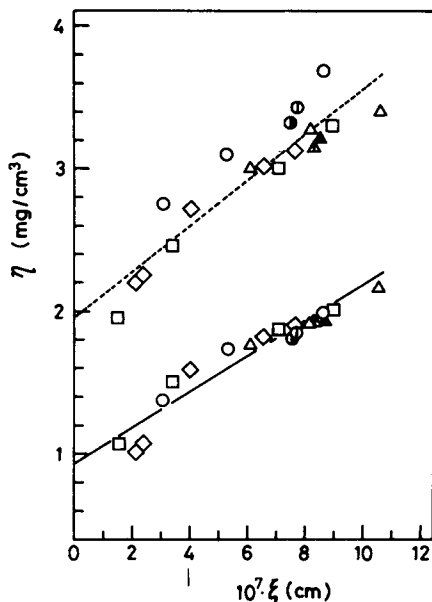


Fig. 7. Test plots based on eq. (9), determined by the least squares fits for the data of Y-7 (—) and PAAB (---). (O, Δ , \square , \diamond) for $p = 0.1$; (\odot , \blacktriangle) for $p = 0.076$; (\bullet) for $p = 0.07$; (\blacktriangle) for $p = 0.061$. These symbols correspond to those utilized in Figure 3.

are plotted in parallel against C_v in Figures 5 and 6. In both cases of dye sorption, the M_e quantities decrease, but the M_s quantities increase with increasing C_v . Since the K_e parameter is, according to the above procedure, assumed to be constant in the whole crystallinity range, the decreases in M_e with increasing C_v is reasonably attributable to the decrease in V_e/V_b . Both volume fractions of the side region and the end region are plotted as a function of C_v in Figure 9, where the values of V_e/V_b decrease monotonically. On the other hand, the in-

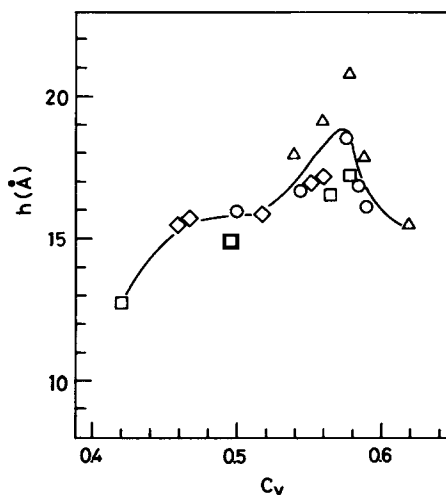


Fig. 8. Change in the thickness of the side region (h) value as a function of crystallinity.

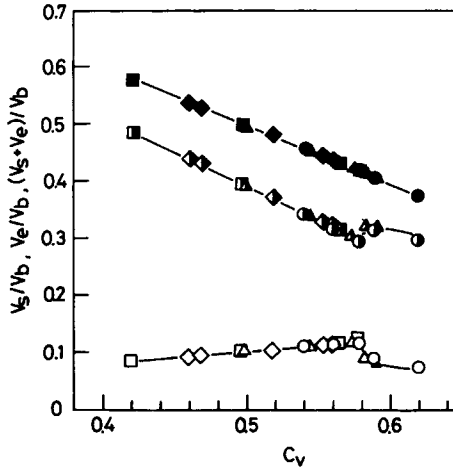


Fig. 9. Change in volume fractions of the end and side regions against volume crystallinity: (●, ▲, ■, ▲) volume fractions of total amorphous region within PP films, i.e., $1 - C_v = (V_s + V_e)/V_b$; (○, △, □, ◇) volume fractions of the end region, V_e/V_b ; (○, △, □, ◇) volume fractions of the side region, V_s/V_b .

crease in M_s below $C_v = 0.58$ is ascribable to the increase in K_s , because the fraction of V_s/V_b shown in Figure 9 remains almost unchanged in this range of C_v . At the higher crystallinity range ($C_v > 0.58$), the quantities of M_s remain almost constant in both cases of dye sorption; this is because the increasing tendency of K_s is counterbalanced by that small decrease in V_s/V_b in this range of C_v , which results from the decrease in the h value. The number of the mosaic block N in the unit volume of the bulk PP film decreases monotonically with an

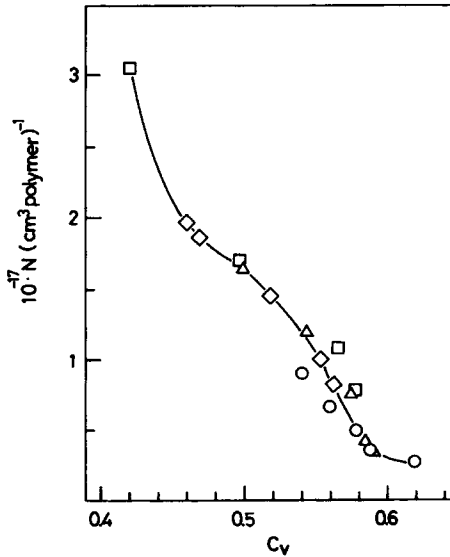


Fig. 10. Change in the average number of the block (N) per unit volume of PP against volume crystallinity. The values of N are calculated by the equation $N = 1/[L_p(l_s + h)^2]$.

increase in C_v , as shown in Figure 10. Therefore, the change in N is, seemingly, independent of variation of M_0 .

Preferential Sorption of Disperse Dyes by the Side Region

In order to compare the sorption of Y-7 by the side region with that of PAAB, it is first necessary to cancel the difference of the dye-bath concentration between the two dyeing cases. The ratio of K_s/K_e becomes independent of the concentration, and this ratio would be qualitatively associated with the molecular shapes of disperse dyes as a linear molecular shape of the dye results in a larger value of K_s/K_e even in the same substrate.⁴

The ratio of K_s/K_e in the present study is plotted against C_v in Figure 11, where the ratio increases monotonically with increasing C_v . Of course, this trend to increase comes from the assumption of eq. (2). Interestingly, the ratios of Y-7 are always larger than those of PAAB in the whole range of crystallinity.

To interpret the above results, we should pay attention to the basic concept of the mosaic block of a crystalline polymer. The "mosaic block model" of Takayanagi and Matsu⁶ corresponds to the findings that the "crystalline phase" consists of microparacrystals (mPC's).¹⁹ Their boundaries have a special structure which is still not known exactly. In crystalline mosaic blocks, the chains fluctuate in such a way as the fluctuation is proportional to the root of the increasing distance from the mPC center. According to the α^* -law,^{20,21} the amorphous side region begins, if this fluctuation reaches a value of 15% of l_{hk0} . This fact may explain why all the samples show the values of $h \cong 15 \text{ \AA}$, independent of their special structure: they seem to follow the α^* -law. This means

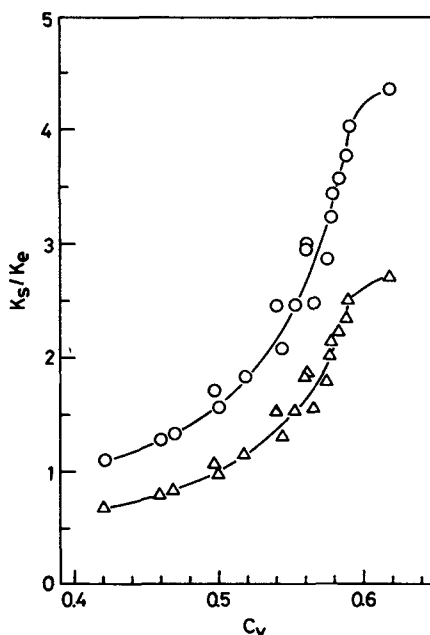


Fig. 11. Changes in the ratio of K_s/K_e for two disperse dyes as functions of volume crystallinity. Symbols indicated are as follows: (O) for Y-7; (Δ) for PAAB.

that, independent of their size, the mPC's always have the same degree of distortions on their boundaries, which allows the dye to penetrate into the grain boundaries. We emphasize, therefore, that in the side region the chains are not coiled but have rather extended conformations. Those chains may build up, so to say, channels with distortions well-defined by α^* -law. In the dynamical equilibrium, the dyes diffuse along these channels. Following the laws of diffusion, the velocity of the penetrant flow is inversely proportional to the l_c of the channel length, and hence, the relation $K_s = l_c \cdot m_s$ can be expected. This is a direct deduction of eq. (2), which until now is "tentatively" assumed on account of the empirically detected linear relation [eq. (9)] between η and ξ .

Since the molecular interaction forces between disperse dye molecules and molecular chains of PP are mainly due to London dispersion forces, we can reasonably consider that long rodlike dye molecules, such as Y-7, have a tendency to bind much more tightly to the chains with extended chain conformations; namely, anisotropic shapes of the dye molecule result in large selectivity of dye sorption coupled with chain conformations.

These results are similar to those obtained from the dyeing experiments of annealed PE,⁴ even though the exact chain conformations of PP in the side region are completely different from those of PE in that region.

References

1. D. N. Marvin, *J. Soc. Dyers Colour.*, **70**, 16 (1954).
2. Y. Mitsuishi and H. Tonami, *Sen-i Gakkaishi*, **20**, 8 (1964) (in Japanese); *Chem. Abstr.*, **62**, 13300e (1965).
3. J. H. Dumbleton, J. P. Bell, and T. Murayama, *J. Appl. Polym. Sci.*, **12**, 2491 (1968).
4. T. Masuko, S. Hasegawa, K. Yonetake, and M. Karasawa, *Makromol. Chem.*, **182**, 2049 (1981).
5. R. Hosemann, W. Wilke, and F. J. Baltá-Calleja, *Acta Crystallogr., Sect. A*, **21**, 118 (1966).
6. M. Takayanagi and T. Matsuo, *J. Macromol. Sci. Phys.*, **B1**, 407 (1967).
7. M. Kojima, *J. Polym. Sci., Part A-2*, **5**, 597 (1967).
8. P. Cella, D. R. Morrow, and J. A. Sauer, *J. Macromol. Sci. Phys.*, **B3**, 33 (1969).
9. H. Shii and K. Ishikawa, *Makromol. Chem.*, **135**, 275 (1970).
10. M. Kojima, *Kobunshi Kagaku*, **25**, 241 (1968) (in Japanese); *Chem. Abstr.*, **69**, 59658y (1968).
11. Y. Wada, Y. Hotta, and R. Suzuki, *J. Polym. Sci., Part C*, **23**, 583 (1968).
12. R. S. Stein and M. B. Rhodes, *J. Appl. Phys.*, **31**, 1873 (1960).
13. A. Weidinger and P. H. Hermans, *Makromol. Chem.*, **50**, 98 (1961).
14. F. Dannuso, G. Moraglio, and G. Natta, *Ind. Plast. Mod.*, **10**, 40 (1958).
15. H. P. Klug and L. E. Alexander, *X-ray Diffraction Procedures*, 2nd ed., Wiley, New York, 1974, Chap. 8, p. 566.
16. A. S. Michaels and H. J. Bixler, *J. Polym. Sci.*, **50**, 413 (1961).
17. H. P. Frank and H. Lehner, *J. Polym. Sci., Part C*, **31**, 193 (1970).
18. H. Shii, K. Ishikawa, and K. Shirakashi, *Kobunshi Kagaku*, **24**, 112 (1967) (in Japanese); *Chem. Abstr.*, **68**, 30311y (1968).
19. H. Čačković, R. Hosemann, and W. Wilke, *Kolloid Z. Z. Polym.*, **234**, 1000 (1969).
20. R. Hosemann, K. Lemm, A. Schonfeld, and W. Wilke, *Kolloid Z. Z. Polym.*, **216/217**, 103 (1967).
21. F. J. Baltá-Calleja and R. Hosemann, *J. Appl. Crystallogr.*, **13**, 521 (1980).

Received May 4, 1981

Accepted April 26, 1983